Actin Controls the Vesicular Fraction of Dopamine Released During Extended Kiss and Run Exocytosis

Raphaël Trouillon[†] and Andrew G. Ewing*[†,‡]

[†]Department of Chemistry and Molecular Biology, University of Gothenburg, S-41296 Gothenburg, Sweden
[‡]Department of Chemical and Biological Engineering, Chalmers University of Technology, S-41296 Gothenburg, Sweden

S *Supporting Information*

ABSTRACT: The effect of latrunculin A, an inhibitor of actin cross-linking, on exocytosis in PC12 cells was investigated with single cell amperometry. This analysis strongly suggests that the actin cytoskeleton might be involved in regulating exocytosis, especially by mediating the constriction of the pore. In an extended kiss-and-run release mode, actin could actually control the fraction of neurotransmitters released by the vesicle. This scaffold appears to contribute, with the lipid membrane and the protein machinery, to the closing dynamics of the pore, in competition with other forces mediating the opening of the exocytotic channel.
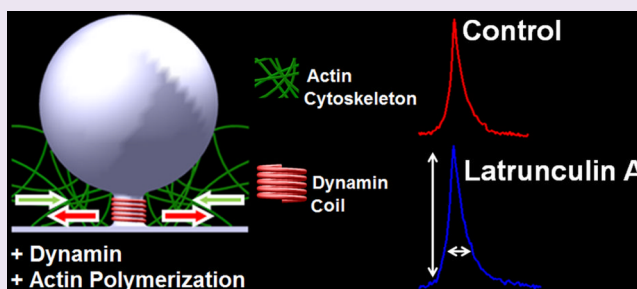
Exocytosis is the main mechanism enabling neuronal communication. This phenomenon is based on the fusion of a neurotransmitter-filled vesicle with the cell membrane, inducing the release of its content into the extracellular space.[1] The released neurotransmitters can then stimulate another neuron, thus enabling signal transmission.

Single cell amperometry can be used for the real-time, quantitative analysis of single exocytotic events.[2−4] In this method, a 5-μm carbon fiber microelectrode is used to oxidize, in a diffusion-limited manner, the neurotransmitters released from the vesicle. This method has been extensively used to investigate the biophysical regulation of exocytosis and the dynamics of the fusion pore formed between the vesicle and the membrane.[5−9] It has also been found that the vesicles might not release all their content during exocytosis, but only about 40%,[10,11] and that the pore does not fully dilate during the course of the event.[12] Partial release, or an extended version of kiss-and-run,[10] might then be the main mode of neuronal communication.[13]

Even though the regulation of the fusion pore on exocytosis has been widely studied, the effects of the physical properties of the extracellular and intracellular environments have not been considered carefully. As shown in Figure 1, the cell is often modeled as a lipid membrane separating two aqueous solutions. However, a cell is actually coated with a glycoprotein matrix and filled with organelles, vesicles, and an actin cytoskeleton. These structures are expected to hinder the dynamics of exocytosis by adding new constraints on the system. For instance, the glycocalyx, a biopolymer coating the cell outer membrane, has recently been found to significantly slow down the exocytotic bolus.[14,15] Inside the cell, the cytoskeleton, especially actin, has been found to be involved in exocytosis.[16] It has been suggested, based on near field microscopic imaging,

that the actin cytoskeleton might constrain the fusion pore,[17] through depolymerization and rearrangement of actin filaments during exocytosis.[18] Thus, we put forward the hypothesis that, for the case of partial release of the vesicular content,[10,11] actin filaments might also be involved in regulating the vesicular fraction released.

In this report, single cell amperometry has been used to investigate the effect of a 30-min incubation with 1 μM latrunculin A (latA), an inhibitor of actin polymerization,[18,19] in HEPES buffer with 0.1% DMSO, on the dynamics and amount of dopamine released during exocytosis in PC12 cells. These experimental results suggest that the actin cytoskeletal scaffold contributes to the closing dynamics of the pore. Release data were also compared to the effect of the dopamine precursor L-DOPA (L-3,4-dihydroxyphenylalanine) to investigate and contrast the role of vesicular packing.[11]

RESULTS AND DISCUSSION

Experimental Design. Several roles have been described for actin in exocytosis.[20,21] It is involved in the transport of the vesicles to the periphery of the cell.[22] Then, the vesicles interact with the dense mesh of actin localized in this region. The actin filaments are here expected to contribute to the priming, docking, and coating of the vesicle during the final prefusion steps.[20,23,24]

In this study we mostly aim at hindering the final actin-vesicle interactions, so that the impact of actin filaments on the characteristics of exocytosis can be elucidated. A decrease in the vesicular trafficking or docking induced by the latA treatment
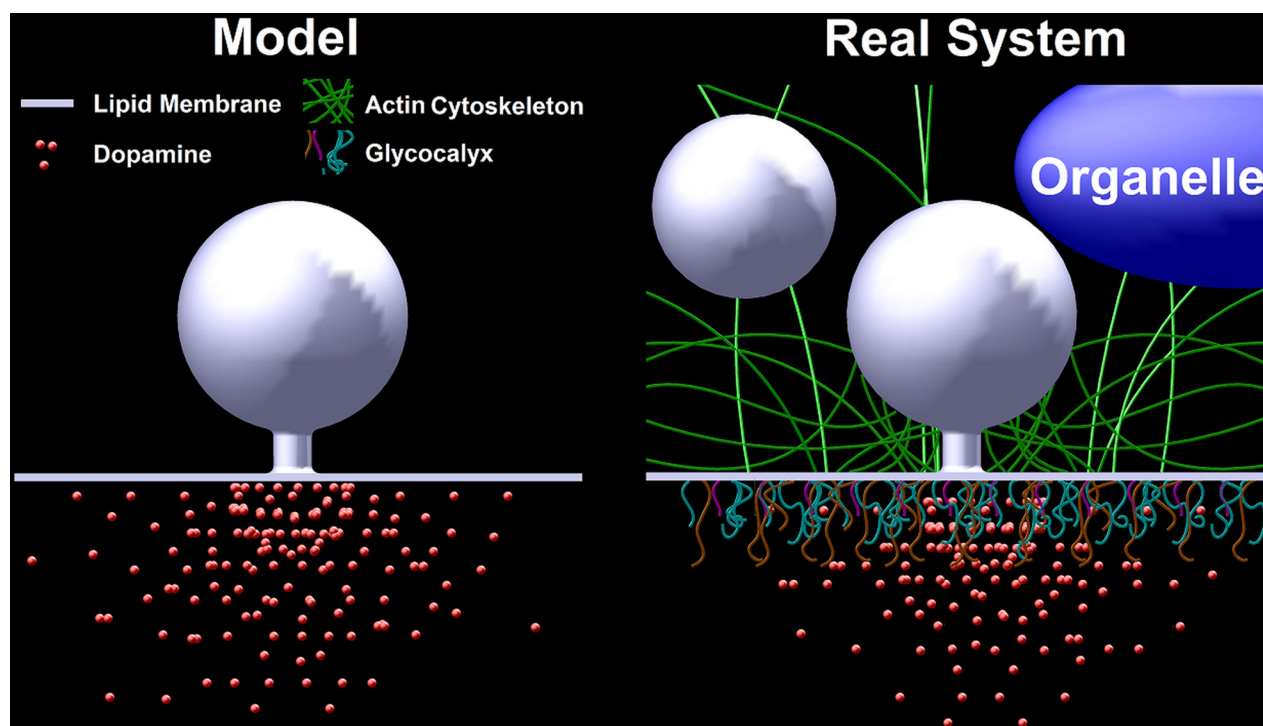
Figure 1. Model *versus* real system. Contrary to the theoretical model where exocytosis occurs in a free aqueous buffer, the intracellular and extracellular spaces are in reality filled with polymers, scaffolds, vesicles, and organelles.

would mostly result in a decrease of the cell exocytotic capability.[25,26] To avoid this, we have used, for the latA exposure, parameters suggested by others (ref 18, 30-min incubation in 1 μM latA). In their report, the authors have observed an increase in the number of exocytotic events recorded per cell after this treatment. A similar effect has been observed in our results, as detailed below. The relatively short (30-min) incubation time guarantees that the impaired vesicle transport and recycling do not have an impact on the experiment. Most of the events recorded in our case then probably arise from vesicles primed and docked to the membrane region before the trafficking properties of the cytoskeleton are abolished by latA. To further ensure the impairments of the vesicular trafficking, recycling, and docking do not hinder our results by depleting the pool of readily available vesicles, each cell was stimulated only once.

Additionally, it has been reported that the effect of latA can be reversed after a few minutes in the absence of the drug.[27] For this reason, the supernatant containing the drug was left over the cells during the measurements. This also minimizes the manipulations of the cells.

Inhibition of Actin Cross-Linking Alters the Exocytotic Response. As shown in Figure 2A, a carbon fiber microelectrode, held at 700 mV, is manipulated to a PC12 cell and positioned against its surface. Exocytosis is triggered by stimulating the cell with a 100 mM K$^+$ solution, eventually leading to the recording of a train of peaks (Figure 3). Several parameters can be obtained from each individual exocytotic event: the 25−75% rise time, t_{rise}; the half peak width, $t_{1/2}$; the 75−25% fall time, t_{fall}; and the number of molecules released, N, obtained by integrating the area under the peak, as shown in Figure 2B.[28] Typical traces obtained from the control (30-min incubation in HEPES buffer with 0.1% DMSO) and latA treatments are shown in Figure 3A. In both cases, the 5-s stimulation is followed by a train of spikes. By looking at the

average events obtained from these traces, it is observed that the latA treatment induces the release of slightly higher and broader events. Additionally, the latA-treated cells display a higher number of events per cell (Figure 3B). This is, in part, due to the larger events obtained after latA incubation, thus facilitating the detection of the peaks. More importantly, exposure to latA almost doubles the amount of neurotransmitters released during the first 30 s of the experiments, as shown in Figure 3C. Altogether, these data suggest that latA might be involved in inducing a larger fusion pore connecting the vesicle to the membrane, already suggesting that actin is involved in the dynamic regulation of exocytosis (Figure 3A).

The peak parameters obtained from these treatments are summarized in Table 1. From these data, it appears that the disruption of the actin scaffold leads to a substantial increase in t_{fall} and in i_p, thus lengthening the time the event takes place. This increase results in a higher amount, N, of molecules released. Assuming an extended kiss-and-run or partial release mechanism, these variations indicate that the cells release a higher fraction of their content after exposure to latA. Additionally, the higher i_p is evidence of a wider pore when the actin matrix is disrupted. This suggests that the actin cytoskeleton is responsible, in part, for constraining the pore dilation, perhaps by increasing the rigidity of the intracellular environment.

Effect of Increased Vesicular Packing. To ensure the results observed after the latA treatment are not due to an increase in vesicular content, the effect of latA has been compared to the results obtained from the 30-min incubation of cells in 100 μM L-DOPA (in HEPES buffer, with 0.1% DMSO). L-DOPA is a synthetic precursor to dopamine, known to increase the vesicular content.[11] Clear exocytotic peaks were again observed upon K$^+$ stimulation (Figure 3A), and the L-DOPA increased the number of events recorded per cell in a magnitude similar to the latA. However, the increase in the
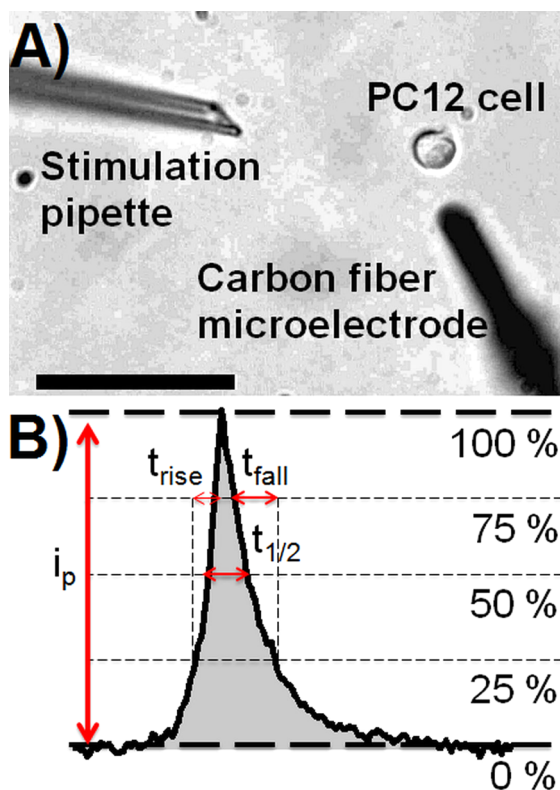
Figure 2. Setup and data processing. (A) Optical micrograph of the setup, showing the stimulation pipet, the PC12 cell, and the microelectrode before it is positioned over the cell (the black bar indicates 50 μm). (B) Scheme showing the different parameters used for the peak analysis. The number of molecules released is evaluated with Faraday's law ($N = Q/nF$), where N is in moles; Q is the area under the peak, shown in gray; n is the number of electrons in the oxidation reaction; and F is Faraday's constant.

total amount of neurotransmitter released was higher than for latA (about 3 times the amount released for the control; see Figure 3C). This fact is in good agreement with the increased vesicular packing induced by the L-DOPA, and thus the effects of the latA and L-DOPA treatments are quantitatively different.

The results obtained comparing the exocytotic peak parameters are presented in Table 1. From these values, it appears that L-DOPA induces a higher increase in N than latA, even for a short 30-min incubation. Additionally, it also increases the characteristic peak times, $t_{1/2}$ and t_{fall}, and i_p. Again, these effects are much more potent than after latA incubation.

However, as shown in Figure 4, the L-DOPA treatment shifts the distribution of N to the right, in a much more dramatic manner than after latA exposure, and small events are not observed anymore. On the contrary, events below 50,000 molecules could still be recorded following latA treatment. This fact suggests that L-DOPA and latA alter the exocytotic peaks *via* different pathways (*i.e.*, vesicular content *vs* pore dynamics, respectively). The same phenomenon is observed with $t_{1/2}$, where L-DOPA treatment completely abolishes the observation of short half-times. Finally, the general distribution of i_p is largely unmodified for the latA treatment and is strongly shifted toward higher values after L-DOPA incubation.

From this analysis, the variations in the peak shape after incubation with L-DOPA are different from what was observed after exposure to latA, indicating that the higher release amount

is not due to an increased vesicular content. The effects of latA and L-DOPA appear to be quantitatively different. The effect of L-DOPA, in good agreement with its reported effect on vesicular content, leads to higher currents, a larger amount released, and a general broadening of the spike. On the other hand, latA does not dramatically change the shape of the peak, apart from a noticeable increase in fall time. From this analysis, it can be reasonably assumed that these two drugs modify different characteristics of the system: L-DOPA increases the size and transmitter load of the vesicle,[11] and latA induces a wider fusion pore (Figures 3A and 4).

Actin Contributes to the Late Kinetic Characteristics of the Pore. To clearly establish the role of actin and to show unambiguously that latA and L-DOPA have different effects on the vesicle, the decaying part of the peak was investigated. Indeed, if the latA treatment induces a wider pore, and somehow impedes the closing of the pore, the shape of this section of the peak will be altered, in comparison to control and to L-DOPA-treated cells. Assuming a partial release mechanism, the peaks obtained from latA-treated cells should be altered to a greater extent by the depletion of the neurotransmitter during partial release as the open pore should allow a higher fraction of release. The pore dynamics should be the same for L-DOPA *versus* control cells, so this should not happen. Indeed, even though L-DOPA is known to alter the fusion pore,[29,30] the vesicular fraction released in L-DOPA-treated cells has been found to be similar to the one observed in control cells.[11] This would therefore indicate that the respective contributions of the pore dynamics and the vesicular depletion are largely comparable in these two cases. In good agreement with this idea, latA and L-DOPA have been found to induce an increase of t_{fall}, but these two treatments have different effects on the distributions of this parameter (Table 1 and Figure 5A). This result indicates that the effect of latA is not due to an increase in vesicular content, but rather to alterations of the fusion pore kinetics.

Previous studies have reported that a double exponential (here referring to a sum of two exponentials), containing a fast and a slow component, might be a better fit than a single exponential to the decaying section of the peak.[28,31−34] Several explanations, such as diffusional filtering, have been suggested, but in this section, we now reconsider the two-exponential fit by assuming an extended kiss-and-run mechanism, *i.e.*, that the pore closes again at the end of the event. According to numerical modeling, in the case of a fixed or opening pore, the asymptotic behavior of the clearance curve is a single exponential.[12] In this case, the asymptotic decay of the exocytotic current is mostly controlled by diffusion of the neurotransmitters through the fusion pore. As a consequence, a perfect single exponential asymptotic behavior strongly hints that the pore does not close again (*i.e.*, is stable or opening) during the course of the exocytotic release. On the basis of this observation, we suggest that the secondary exponential term is an indication of the last possible case, *i.e.*, the collapse of the pore, the secondary exponential being related to the closing kinetics of the lipid nanotube.[35] A last possibility, in the case of a single exponential decay, is that this part of the peak is controlled by the pore constriction only. This would necessarily mean that the content of the vesicle remains almost stable and hence that only a small fraction of transmitter is released. This would be in complete contradiction with the finding that about 40% of the content is released.[10,11] We therefore consider two situations: a purely diffusive case, where the decay is controlled
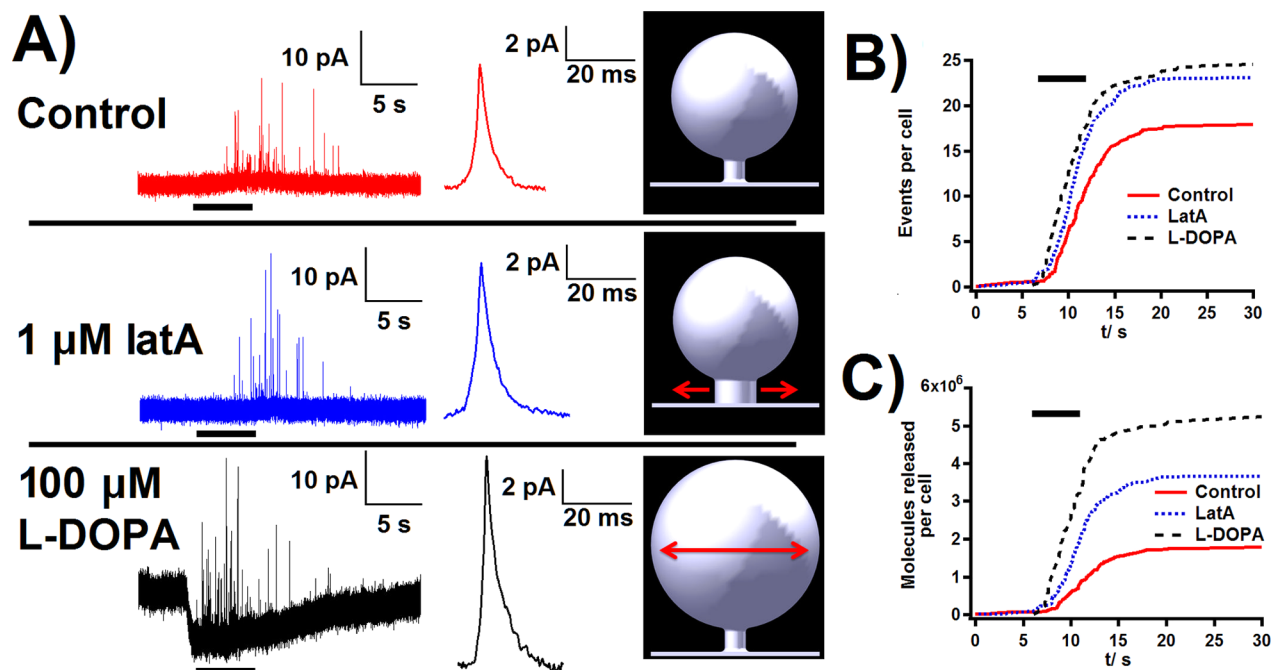
Figure 3. (A) Typical traces obtained from control (top), 1 μM latA-treated (center), and 100 μM L-DOPA-treated (bottom) cells. The black bar indicates the 5-s K⁺ stimulation. On the right side of each trace, the corresponding average peak and a representation of the suggested exocytotic system corresponding to each treatment, with latA widening the fusion pore and L-DOPA generating larger vesicles,[11,29,30] are shown. (B) Average cumulative number of events recorded and C) average cumulative number of molecules released per cell for the first 30 s of the experiment for the control (10 cells, 216 peaks), 1 μM latA (10 cells, 291 peaks), and 100 μM L-DOPA (5 cells, 122 peaks) treatments.

Table 1. Experimental Results for t_{rise}, $t_{1/2}$, t_{fall}, i_p, and N Obtained from K⁺-Stimulated PC12 Cells[a]

treatment	t_{rise} (ms)	$t_{1/2}$ (ms)	t_{fall} (ms)	i_p (pA)	$N/10^3$ molecules
control	0.7 (0.4–1.2)	3.0 (1.9–4.1)	2.4 (1.5–3.7)	6.5 (4.2–11.7)	91 (63–118)
1 μM latA	0.7 (0.4–1.2)	3.3 (2.3–4.3)	2.8 (1.8–4.0)	8.3 (4.8–13.8)	127 (91–193)
variation	+1% (0.07804)	+12% (0.0299)	+16% (0.0079)	+27% (0.0077)	+40% (0.0000)
100 μM L-DOPA	0.6 (0.4–0.9)	4.3 (3.1–5.3)	4.8 (3.3–6.3)	8.5 (6.7–12.9)	160 (124–237)
variation	−14% (0.2622)	+44% (0.0000)	+98% (0.0000)	+32% (0.0000)	+77% (0.0000)

[a]Comparing control (10 cells, 216 peaks) to exposure to 1 μM latA (10 cells, 291 peaks) and to 100 μM L-DOPA treatments (5 cells, 122 peaks). The data are presented as median (1st quartile–3rd quartile). The variation of the median in comparison to the control is also reported. The pairs of data sets were compared using a two-tailed Wilcoxon–Mann–Whitney rank-sum test, and the result is indicated, between brackets, next to the variation of the median. Means are reported in the Supporting Information.

by the diffusion of the neurotransmitters out of the vesicle (single exponential), and a second case where this efflux is also constrained by a closing pore (double exponential).

As a consequence, the decay of all of the peaks observed in our experiments was fit with a double decaying exponential to further understand the mechanisms controlling the fusion pore:

$$f(t) = A_1 e^{-(t-t_0)/T_1} + A_2 e^{-(t-t_0)/T_2} \qquad (1)$$

where t_0 is the starting time of the decay, and T_1 and T_2 are the characteristic decay times (with $T_1 \leq T_2$). If a single exponential provides a better fit, a criterion would be that $T_1 \approx T_2$.

The normalized distance, d, between the point (T_1, T_2) and the line describing the identity function is used as a criterion for evaluating whether a decay is better fit with a single or double exponential (Figure 5B). If d is small, then the $T_1 \approx T_2$ condition is satisfied and this peak is better fit with a single exponential. The normalized distance d is calculated as follows:

$$d(T_1, T_2) = \frac{T_2 - T_1}{\sqrt{2}\, \|(T_1, T_2)\|} = \sin\theta \qquad (2)$$

where $\|(T_1, T_2)\|$ is the norm of the vector (T_1, T_2), and θ is the angle formed by the vectors (T_1, T_2) and $(1, 1)$. This parameter was calculated for every peak. Indeed, the main goal of our method is to discriminate those peaks better fit with a double exponential from those better fit with a single exponential. As shown in eq 1, four parameters are obtained from our fitting, and all of them are expected to carry specific information. The factors A_1 and A_2 are simply indicative of the scaling of the two exponentials and do not determine the nature of the curve (i.e., single or double exponential). However, by focusing on the two characteristic times T_1 and T_2 and using the $T_1 \approx T_2$ criterion and the normalized distance d, it is then possible to reduce the problem to these two variables, to address the single versus double exponential problem.

Figure 5C shows the cumulative histograms obtained for d, for each treatment. The y-axis shows the calculated d, and the x-axis the fraction of the peak population whose d is below this value. For example, for the control treatment, about 50% of the peaks show a d below 0.1. Each of the histograms has then been fit with a sigmoid. The latA treatment displaces the center of
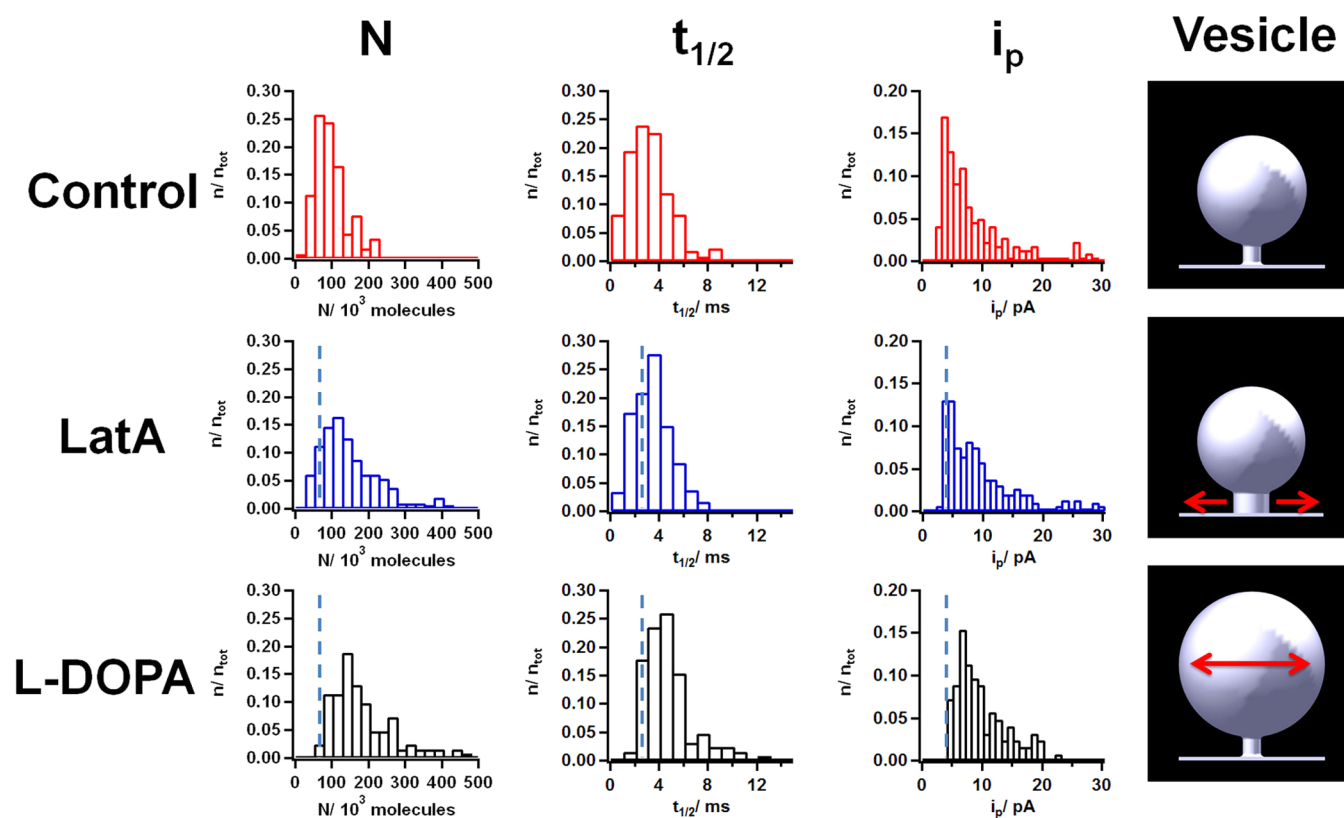
Figure 4. Histograms for the number of molecules released, N, the half-time, $t_{1/2}$, and the peak current, i_p, for the control, 1 μM latA, and 100 μM L-DOPA treatments; the blue dotted bars indicate the position of the maximum of the distribution for control. From the data shown on the histograms, 1 μM latA is interpreted to induce a wider pore opening, and the 100 μM L-DOPA treatment is known to increase the vesicular size and content.[11,29,30] The right side of the figure shows a model of the exocytotic vesicle, corresponding to each treatment, with latA widening the fusion pore and L-DOPA generating larger vesicles.
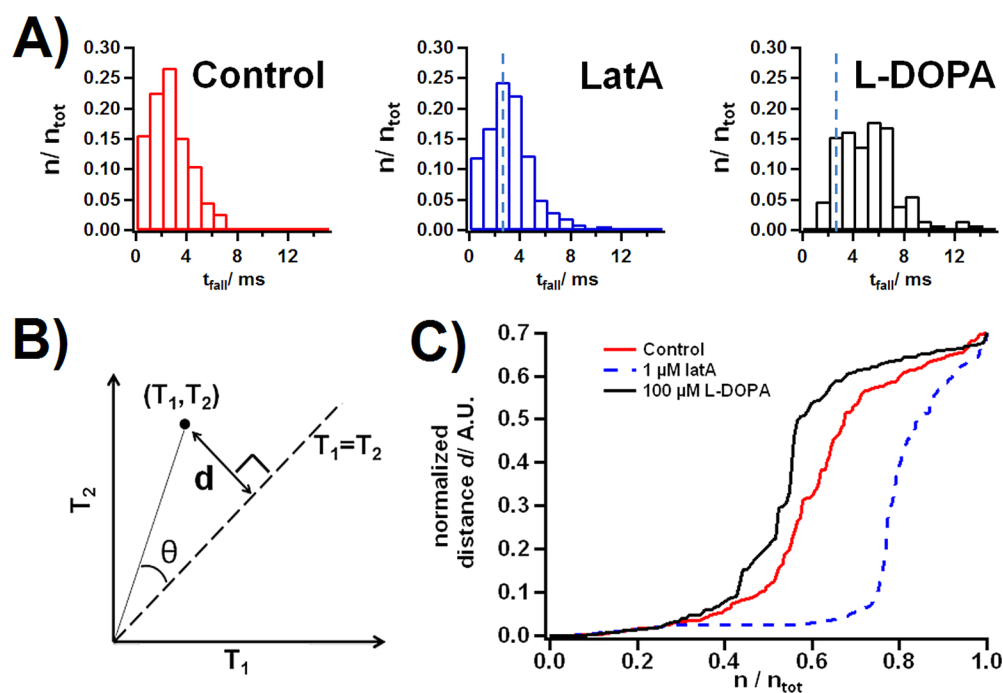
Figure 5. Single *versus* double exponential analysis. (A) Histograms of the fall time t_{fall}, for the control, 1 μM latA and 100 μM L-DOPA treatments; the blue dotted bar indicates the position of the maximum of the distribution for the control case. (B) Scheme defining the normalized distance d to the "$T_1 = T_2$" line used in the analysis. (C) Single *versus* double exponential analysis showing the cumulative histograms of the normalized distance, d, for the control, 1 μM latA, and 100 μM L-DOPA treatments.

this sigmoid to the right (control, 0.60; 1 μM latA, 0.79). This indicates that the latA treatment reduces the prevalence of high d values, thus favoring the single exponential decay. As the second exponential fitting is considered to be evidence for pore constriction, this result suggests, in good agreement with the increased t_{fall} value, that disruption of the actin network reduces the rate of contraction of the pore during the decay of the peak.

The single *versus* double exponential analysis was repeated for the L-DOPA-treated cells. The result of this analysis is shown in Figure 5C. Even though both latA and L-DOPA induce larger, broader, and higher peaks, they have opposite effects on the distribution of the normalized distance, d. L-DOPA increases this occurrence of double exponential decays, thus indicating that the effect of the pore on the shape of the peak is more important in comparison to control. This increase probably indicates a stronger contribution of the closing of the pore on the vesicular efflux, in this case where the vesicular content is 50% higher than for control.[11] This is also an important control to establish the viability of our method. Indeed, it could be possible that the double exponential arise from another factor than the competition between release and pore constriction. For instance, one exponential could be from the exocytotic signal, and the other one from the noise. As the signal-to-noise ratios are comparable in the latA and L-DOPA cases, the different single *versus* double exponential distributions are therefore induced by specific characteristics of the exocytotic peaks. This result supports the viability of the method presented here indicating biological factors.

A rigorous analysis of the exact physical meaning of T_1 and T_2 exceeds the scope of the present study, but qualitative considerations can be brought to the discussion. As explained above, we assume that two distinct phenomena, the depletion of the vesicle and the constriction of the pore, are described by T_1 and T_2. The current measured at the electrode results from the efflux of neurotransmitters out of the vesicle, *via* the fusion pore, driven by the chemical potential energy of the higher concentration of neurotransmitter inside the vesicle. Hence, for the pore constriction to have an effect on the vesicular efflux, the rate of constriction of the pore has to be faster than the rate of diffusion out of the vesicle. From this observation, we can assume that, as $T_1 \leq T_2$ by definition, T_1 is characteristic of the pore constriction and T_2 of the depletion of the vesicular content.

As shown in Table 2, for the peaks better fit with a double exponential (*i.e.*, the ones corresponding to $d > 0.5$), the experimental values for T_1 have been found to be increased by both the latA and L-DOPA treatments, in comparison to control. However, only the L-DOPA treatment was found to significantly increase T_2. On the basis of the qualitative analysis of the roles of T_1 and T_2 and the fact that T_1 may be principally indicative of the constriction of the pore, these data support the idea that the constriction of the pore is slower when the cells are exposed to latA. Thus, the rate of depletion of the vesicular content is, in comparison, largely unaltered, and the intact actin network appears to participate in the closing of the fusion pore. The observation that both T_1 (constriction of the pore) and T_2 (rate of depletion of the vesicular content) are changed by the L-DOPA treatment can be explained by the increased vesicular packing. Due to the higher amount of material, it will take a longer time to deplete the cell (higher T_2), and the higher tension in the vesicle membrane, due to the vesicle swelling, is expected to alter the properties of the pore (higher T_1, ref 29).

**Table 2. Experimental Results for T_1 and T_2 Obtained from K$^+$-Stimulated PC12 Cells, for Peaks with $d > 0.5$[a]**

treatment	T_1 (ms)	T_2 (ms)
control	0.9 (0.5–1.5)	8.4 (5.6–11.7)
1 μM latA	1.8 (0.9–2.2)	11.9 (8.0–17.3)
variation	+91% (0.0004)	+42% (0.0109)
100 μM L-DOPA	1.5 (1.1–2.3)	14.4 (11.5–23.6)
variation	+65% (0.0001)	+72% (0.0000)

[a]Comparing control (10 cells, 71 peaks) to exposure to 1 μM latA (10 cells, 46 peaks) or to 100 μM L-DOPA (5 cells, 53 peaks). The data are presented as median (1st quartile−3rd quartile). The values reported in this table are the ones obtained for the peaks better fit with a double exponential. The criterion of selection for these peaks was $d >$ 0.5. The variation of the median in comparison to the control is reported. The pairs of data sets were compared using a two-tailed Wilcoxon−Mann−Whitney rank-sum test, and the result is indicated, between brackets, next to the variation of the median.

One of the main variations in the peak characteristics after the latA treatment is the observed increase in peak fall time. The decaying part of the peak is expected to contain some information about the closing of the fusion pore in extended kiss-and-run release.[10] In this case, the increased fall time is evidence that the inhibition of actin polymerization increases the lifetime of the pore and slows down the collapse of the pore. This strongly suggests that actin is an important factor in the closing dynamics of the lipid pore. This observation agrees with the results of the single *versus* double exponential analysis. The comparison of the peaks obtained with the latA treatments to the those obtained after the L-DOPA incubation is particularly informative as these treatments lead to an increased release amount but have opposite effects on the T_1 and T_2 distributions. This further demonstrates that latA and L-DOPA increase the release amount *via* different pathways.

Proposed Role for Actin in Exocytosis. The results presented here underline the role of actin polymerization in controlling the dynamics of exocytotic release. More precisely, inhibition of actin leads to an increase in the amount of molecules released and to a decrease in the rate of closing of the fusion pore. Modulation of the dynamics of exocytosis by the cytoskeleton, although controversial, in fact agrees with several reports of release heterogeneity over the cell surface.[36−40] Furthermore, it has been found that events measured at the base of the cell are different from the ones made at its apex.[41,42] In light of the results presented here, it is reasonable to suggest that this heterogeneity might arise from the structure of the cytoskeleton.

Exocytosis was initially thought to lead to the full distension of the vesicle and to its integration into the cell membrane. However, several studies now support the occurrence of a mechanism that more resembles an extended kiss-and-run process, where only a fraction of the vesicular content is released.[43,44] In good agreement with this hypothesis, PC12 cell vesicles release only 40% of their content during exocytosis.[10,11] In our study, a 40% increase of the median of the amount released is observed (this corresponds to a 51% increase of the mean release; see Table S1 in the Supporting Information). The probability to obtain large events (>200 000 molecules released) is also increased (Figure 4). As this phenomenon might be induced by a higher vesicular packing, the latA results have also been compared to the effect of L-DOPA.[11] It was then found that a latA-induced increase in vesicular packing is unlikely and that the observed increase in the amount of
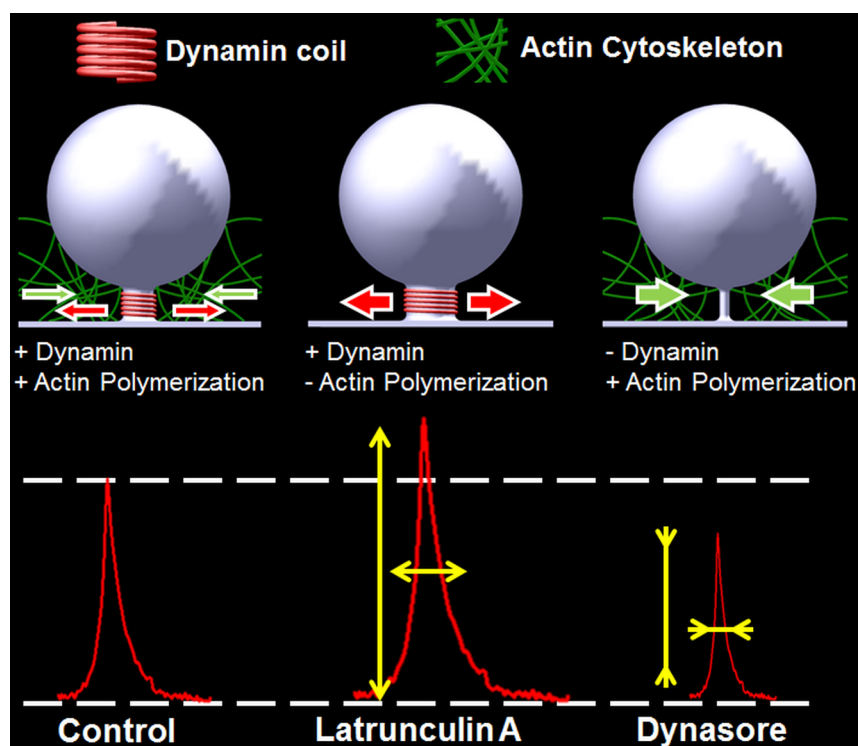
Figure 6. Proposed scheme for the contribution of dynamin and actin to exocytosis. Actin appears to force the closing of the pore, whereas dynamin promotes its opening.[35] The resulting typical amperometric spikes are presented below (not drawn to scale). Exposure to latrunculin A induces higher, wider peaks, and inhibition of the GTPase activity of dynamin with the inhibitor dynasore induces shorter, narrow peaks.[35]

molecules released is probably due to an alteration of the pore dynamics. Altogether, the analysis presented indicates that the inhibition of actin leads to a reduced contribution of the fusion pore on the recorded exocytotic peak. We thus suggest that actin is involved in regulating the closing dynamics of the pore, thus controlling the decaying part of the amperometric peak. These findings strongly support the theory of partial release at PC12 cells and that actin is involved in regulating the amount of vesicular content released during extended kiss-and-run exocytosis.

Interestingly, actin is known to interact with several membrane-shaping chemical motors, such as dynamin.[45−47] This GTPase has recently been found to, in part, regulate the fate of the fusion pore, probably by mediating its dilation.[35,48−50] Together with the data presented here, we suggest that the regulation of the fusion pore dynamics is a competitive process between different mechanochemical transducers, as summarized in Figure 6. In this case, dynamin, at least in part, promotes the opening of the pore, and actin its closure. The composition of the lipid membrane also plays a critical part.[6,7] However, this list is not exhaustive, as other polymers, proteins, or lipid structures might clearly contribute to this highly dynamic and competitive process.

From these results, we suggest that in PC12 cells the actin cytoskeletal scaffold contributes, probably with the lipid membrane and the protein machinery, to the closing dynamics of the pore. Thus, the cytoskeleton likely regulates the vesicular fraction released in an extended kiss-and-run mode.[10−12] We have recently shown that dynamin is involved in holding open the pore during exocytosis,[35] so it appears likely that actin and dynamin complement each other in balancing and controlling release during an open and closed exocytosis process.

METHODS

The experimental details and procedures for the cell culture, the electrochemical measurements, and the data processing are provided as Supporting Information.

ASSOCIATED CONTENT

Ⓢ Supporting Information

Details on our experimental procedures and two additional tables where the mean of the data was computed in place of the median. This material is available free of charge *via* the Internet at http://pubs.acs.org.

AUTHOR INFORMATION

Corresponding Author
*E-mail: andrew.ewing@chem.gu.se.
Notes
The authors declare no competing financial interest.

ACKNOWLEDGMENTS

REFERENCES

(1) Heuser, J. E., Reese, T. S., Dennis, M. J., Jan, Y., Jan, L., and Evans, L. (1979) Synaptic vesicle exocytosis captured by quick freezing and correlated with quantal transmitter release. *J. Cell Biol.* 81, 275−300.
(2) Wightman, R. M., Jankowski, J. A., Kennedy, R. T., Kawagoe, K. T., Schroeder, T. J., Leszczyszyn, D. J., Near, J. A., Diliberto, E. J., Jr, and Viveros, O. H. (1991) Temporally resolved catecholamine spikes

correspond to single vesicle release from individual chromaffin cells. *Proc. Natl. Acad. Sci. U.S.A. 88*, 10754–10758.

(3) Trouillon, R., Passarelli, M. K., Wang, J., Kurczy, M. E., and Ewing, A. G. (2013) Chemical analysis of single cells. *Anal. Chem. 85*, 522–542.

(4) Lin, Y., Trouillon, R., Safina, G., and Ewing, A. G. (2011) Chemical analysis of single cells. *Anal. Chem. 83*, 4369–4392.

(5) Sulzer, D., and Pothos, E. N. (2000) Regulation of quantal size by presynaptic mechanisms. *Rev. Neurosci. 11*, 159–212.

(6) Amatore, C., Arbault, S., Bouret, Y., Guille, M., Lemaître, F., and Verchier, Y. (2006) Regulation of exocytosis in chromaffin cells by trans-insertion of lysophosphatidylcholine and arachidonic acid into the outer leaflet of the cell membrane. *ChemBioChem 7*, 1998–2003.

(7) Uchiyama, Y., Maxson, M. M., Sawada, T., Nakano, A., and Ewing, A. G. (2007) Phospholipid mediated plasticity in exocytosis observed in PC12 cells. *Brain Res. 1151*, 46–54.

(8) Borisovska, M., Zhao, Y., Tsytsyura, Y., Glyvuk, N., Takamori, S., Matti, U., Rettig, J., Südhof, T., and Bruns, D. (2005) v-SNAREs control exocytosis of vesicles from priming to fusion. *EMBO J. 24*, 2114–2126.

(9) Simonsson, L., Kurczy, M. E., Trouillon, R., Hook, F., and Cans, A.-S. (2012) A functioning artificial secretory cell. *Sci. Rep.*, DOI: 10.1038/srep00824.

(10) Mellander, L. J., Trouillon, R., Svensson, M. I., and Ewing, A. G. (2012) Amperometric post spike feet reveal most exocytosis is via extended kiss-and-run fusion. *Sci. Rep. 2*, 907.

(11) Omiatek, D. M., Dong, Y., Heien, M. L., and Ewing, A. G. (2010) Only a fraction of quantal content is released during exocytosis as revealed by electrochemical cytometry of secretory vesicles. *ACS Chem. Neurosci. 1*, 234–245.

(12) Amatore, C., Oleinick, A. I., and Svir, I. (2010) Reconstruction of aperture functions during full fusion in vesicular exocytosis of neurotransmitters. *ChempPhysChem 11*, 159–174.

(13) Harata, N. C., Aravanis, A. M., and Tsien, R. W. (2006) Kiss-and-run and full-collapse fusion as modes of exo-endocytosis in neurosecretion. *J. Neurochem. 97*, 1546–1570.

(14) Trouillon, R., and Ewing, A. G. (2013) Single cell amperometry reveals glycocalyx hinders the release of neurotransmitters during exocytosis. *Anal. Chem. 85*, 4822–4828.

(15) Trouillon, R., Lin, Y., Mellander, L. J., Keighron, J. D., and Ewing, A. G. (2013) Evaluating the diffusion coefficient of dopamine at the cell surface during amperometric detection: disk vs ring microelectrodes. *Anal. Chem. 85*, 6421–6428.

(16) Ge, S., White, J. G., and Haynes, C. L. (2012) Cytoskeletal F-actin, not the circumferential coil of microtubules, regulates platelet dense-body granule secretion. *Platelets 23*, 259–263.

(17) Wang, J., and Richards, D. A. (2011) Spatial regulation of exocytic site and vesicle mobilization by the actin cytoskeleton. *PLoS One 6*, e29162.

(18) Guzmán, R. E., Bolaños, P., Delgado, A., Rojas, H., DiPolo, R., Caputo, C., and Jaffe, E. H. (2007) Depolymerisation and rearrangement of actin filaments during exocytosis in rat peritoneal mast cells: involvement of ryanodine-sensitive calcium stores. *Pfluegers Arch. Eur. J. Physiol. 454*, 131–141.

(19) Coué, M., Brenner, S. L., Spector, I., and Korn, E. D. (1987) Inhibition of actin polymerization by latrunculin A. *FEBS Lett. 213*, 316–318.

(20) Trifaró, J.-M., Gasman, S., and Gutiérrez, L. M. (2008) Cytoskeletal control of vesicle transport and exocytosis in chromaffin cells. *Acta Physiol. 192*, 165–172.

(21) Nightingale, T. D., Cutler, D. F., and Cramer, L. P. (2012) Actin coats and rings promote regulated exocytosis. *Trends Cell Biol. 22*, 329–337.

(22) Schuh, M. (2011) An actin-dependent mechanism for long-range vesicle transport. *Nat. Cell Biol. 13*, 1431–1436.

(23) Miklavc, P., Wittekindt, O. H., Felder, E., and Dietl, P. (2009) Ca^{2+}-dependent actin coating of lamellar bodies after exocytotic fusion: a prerequisite for content release or kiss-and-run. *Ann. N. Y. Acad. Sci. 1152*, 43–52.

(24) Jerdeva, G. V., Wu, K., Yarber, F. A., Rhodes, C. J., Kalman, D., Schechter, J. E., and Hamm-Alvarez, S. F. (2005) Actin and non-muscle myosin II facilitate apical exocytosis of tear proteins in rabbit lacrimal acinar epithelial cells. *J. Cell Sci. 118*, 4797–4812.

(25) Richards, D. A., Rizzoli, S. O., and Betz, W. J. (2004) Effects of wortmannin and latrunculin A on slow endocytosis at the frog neuromuscular junction. *J. Physiol. 557*, 77–91.

(26) Omata, W., Shibata, H., Li, L., Takata, K., and Kojima, I. (2000) Actin filaments play a critical role in insulin-induced exocytotic recruitment but not in endocytosis of GLUT4 in isolated rat adipocytes. *Biochem. J. 346* (Pt 2), 321–328.

(27) Carnell, M., Zech, T., Calaminus, S. D., Ura, S., Hagedorn, M., Johnston, S. A., May, R. C., Soldati, T., Machesky, L. M., and Insall, R. H. (2011) Actin polymerization driven by WASH causes V-ATPase retrieval and vesicle neutralization before exocytosis. *J. Cell Biol. 193*, 831–839.

(28) Mosharov, E. V., and Sulzer, D. (2005) Analysis of exocytotic events recorded by amperometry. *Nat. Methods 2*, 651–658.

(29) Sombers, L. A., Hanchar, H. J., Colliver, T. L., Wittenberg, N., Cans, A., Arbault, S., Amatore, C., and Ewing, A. G. (2004) The effects of vesicular volume on secretion through the fusion pore in exocytotic release from PC12 cells. *J. Neurosci. 24*, 303–309.

(30) Colliver, T. L., Pyott, S. J., Achalabun, M., and Ewing, A. G. (2000) VMAT-Mediated changes in quantal size and vesicular volume. *J. Neurosci. 20*, 5276–5282.

(31) Wang, C. T., Grishanin, R., Earles, C. A., Chang, P. Y., Martin, T. F., Chapman, E. R., and Jackson, M. B. (2001) Synaptotagmin modulation of fusion pore kinetics in regulated exocytosis of dense-core vesicles. *Science 294*, 1111–1115.

(32) Fang, Q., Berberian, K., Gong, L.-W., Hafez, I., Sørensen, J. B., and Lindau, M. (2008) The role of the C terminus of the SNARE protein SNAP-25 in fusion pore opening and a model for fusion pore mechanics. *Proc. Natl. Acad. Sci. U.S.A. 105*, 15388–15392.

(33) Zhu, D., Zhou, W., Liang, T., Yang, F., Zhang, R.-Y., Wu, Z.-X., and Xu, T. (2007) Synaptotagmin I and IX function redundantly in controlling fusion pore of large dense core vesicles. *Biochem. Biophys. Res. Commun. 361*, 922–927.

(34) Koh, T.-W., and Bellen, H. J. (2003) Synaptotagmin I, a Ca^{2+} sensor for neurotransmitter release. *Trends Neurosci. 26*, 413–422.

(35) Trouillon, R., and Ewing, A. G. (2013) Amperometric measurements at cells support a role for dynamin in the dilation of the fusion pore during exocytosis. *ChemPhysChem 14*, 2295–2301.

(36) Schroeder, T. J., Jankowski, J. A., Senyshyn, J., Holz, R. W., and Wightman, R. M. (1994) Zones of exocytotic release on bovine adrenal medullary cells in culture. *J. Biol. Chem. 269*, 17215–17220.

(37) Zhang, B., Adams, K. L., Luber, S. J., Eves, D. J., Heien, M. L., and Ewing, A. G. (2008) Spatially and temporally resolved single-cell exocytosis utilizing individually addressable carbon microelectrode arrays. *Anal. Chem. 80*, 1394–1400.

(38) Zhang, B., Heien, M. L. A. V., Santillo, M. F., Mellander, L., and Ewing, A. G. (2011) Temporal resolution in electrochemical imaging on single PC12 cells using amperometry and voltammetry at microelectrode arrays. *Anal. Chem. 83*, 571–577.

(39) Lin, Y., Trouillon, R., Svensson, M. I., Keighron, J. D., Cans, A.-S., and Ewing, A. G. (2012) Carbon-ring microelectrode arrays for electrochemical imaging of single cell exocytosis: fabrication and characterization. *Anal. Chem. 84*, 2949–2954.

(40) Wang, J., Trouillon, R., Lin, Y., Svensson, M. I., and Ewing, A. G. (2013) Individually addressable thin-film ultramicroelectrode array for spatial measurements of single vesicle release. *Anal. Chem. 85*, 5600–5608.

(41) Amatore, C., Arbault, S., Lemaître, F., and Verchier, Y. (2007) Comparison of apex and bottom secretion efficiency at chromaffin cells as measured by amperometry. *Biophys. Chem. 127*, 165–171.

(42) Meunier, A., Fulcrand, R., Darchen, F., Guille Collignon, M., Lemaître, F., and Amatore, C. (2012) Indium tin oxide devices for amperometric detection of vesicular release by single cells. *Biophys. Chem. 162*, 14–21.

(43) Alés, E., Tabares, L., Poyato, J. M., Valero, V., Lindau, M., and Alvarez de Toledo, G. (1999) High calcium concentrations shift the mode of exocytosis to the kiss-and-run mechanism. *Nat. Cell Biol. 1*, 40−44.

(44) Fesce, R., Grohovaz, F., Valtorta, F., and Meldolesi, J. (1994) Neurotransmitter release: fusion or "kiss-and-run"? *Trends Cell Biol. 4*, 1−4.

(45) Gu, C., Yaddanapudi, S., Weins, A., Osborn, T., Reiser, J., Pollak, M., Hartwig, J., and Sever, S. (2010) Direct dynamin-actin interactions regulate the actin cytoskeleton. *EMBO J. 29*, 3593−3606.

(46) Orth, J. D., and McNiven, M. A. (2003) Dynamin at the actin-membrane interface. *Curr. Opin. Cell Biol. 15*, 31−39.

(47) Pelkmans, L., Püntener, D., and Helenius, A. (2002) Local actin polymerization and dynamin recruitment in SV40-induced internalization of caveolae. *Science 296*, 535−539.

(48) González-Jamett, A. M., Báez-Matus, X., Hevia, M. A., Guerra, M. J., Olivares, M. J., Martínez, A. D., Neely, A., and Cárdenas, A. M. (2010) The association of dynamin with synaptophysin regulates quantal size and duration of exocytotic events in chromaffin cells. *J. Neurosci. Off. J. Soc. Neurosci. 30*, 10683−10691.

(49) Ramachandran, R., and Schmid, S. L. (2008) Real-time detection reveals that effectors couple dynamin's GTP-dependent conformational changes to the membrane. *EMBO J. 27*, 27−37.

(50) Anantharam, A., Axelrod, D., and Holz, R. W. (2012) Real-time imaging of plasma membrane deformations reveals pre-fusion membrane curvature changes and a role for dynamin in the regulation of fusion pore expansion. *J. Neurochem. 122*, 661−671.